

## Supplemental Methods

**Patients selection.** Patients were diagnosed with primary ICH in National Taiwan University Hospital (NTUH) from September 2014 to March 2017 after secondary etiologies, including underlying structural vascular pathology (arteriovenous malformation, cavernoma), coagulopathy, anticoagulation or any other vascular cause were ruled out. Because MRI and SWI are mandatory to detect CMBs and to determine the severity of underlying SVD, we retrospectively collected data from (1) patients admitted for symptomatic primary ICH with brain MRI and SWI, retrieved from the prospective NTUH stroke registry (n=180) (2) patients referred from other hospitals and participated in the MRI and amyloid PET study at the NTUH stroke clinic (n=34).<sup>1</sup> Supplementary figure I showed the flow chart of patient enrollment. In the NTUH stroke registry, primary ICH patients without MRI/SWI studies (n=351) had similar age and sex distribution as patients who underwent MRI/SWI studies (age  $61.1 \pm 18.1$  years vs  $63.3 \pm 13.6$  years,  $p=0.105$ ; male 64.1% vs 63.9%,  $p=0.964$ ). Patients with lobar ICH involving the cerebral cortex and underlying WM with or without strictly lobar CMBs or cortical superficial siderosis (cSS) were coded as probable (n=15) or possible (n=9) CAA-ICH by the modified Boston criteria.<sup>2</sup> Patients with HTN-ICH were defined as patients with ICH in the basal ganglia, thalamus, or infratentorial region (deep locations) with or without deep CMB but no lobar CMB (n=86). Primary cerebellar ICH (n=11) were not included for analyses. To increase the diagnostic accuracy for the underlying dominant microangiopathy, patients with a combination of mixed lobar and deep macrobleed/microbleed were excluded (n=104). A subgroup of 36 patients (15 CAA-ICH, 21 HTN-ICH) without overt cognitive impairment also received a <sup>11</sup>C-PiB PET to determine brain amyloid retention. As already described, baseline clinical data collection was performed through reviewing medical records comprehensively.<sup>1,3</sup>

**MRI analyses.** Images were obtained using 3T MRI scanners (Siemens Verio, TIM, or mMR).

SWI acquisition was performed with a T2\*-weighted gradient echo sequence with flip angle 15°, TR/TE = 28/20 ms, matrix number = 221x320, FOV = 23 cm, slice thickness = 1.6 mm. SWI and minimum intensity projection images were acquired by in-line post-processing of magnitude and phase images, and these post-processed images were used for the evaluation of the imaging findings. Other conventional imaging protocols included T1-weighted, T2-weighted, and fluid-attenuated inversion recovery (FLAIR) imaging. The median time from ICH occurrence to brain MRI study was 4 (1-127) days, and was significantly longer for patients from outside hospital than for patients admitted in NTUH (279 [136-675] vs. 2 [1-14],  $p < 0.001$ ).

The presence and number of CMBs were evaluated on SWI as previously described.<sup>4</sup> Cortical superficial siderosis (cSS) was defined as homogenous curvilinear signal loss on SWI outlining the superficial layers of the cerebral cortex.<sup>5</sup> Enlarged perivascular spaces (EPVS) were defined as sharply delineated structures on T2-weighted imaging, measuring  $< 3$  mm following the course of perforating or medullary vessels.<sup>6</sup> The number of EPVS (one side of the brain with more severe involvement) was measured in BG and centrum semiovale and we pre-specified a dichotomized classification of EPVS degree as high (score  $> 20$ ) or low (score  $\leq 20$ ).<sup>6</sup> WMH volume was calculated using an in-house semi-automated algorithm. After registering the T2-FLAIR volume to the T1-weighted volume, a minimum intensity threshold of 1.5 standard deviations was applied, similarly to a previously published method.<sup>7, 8</sup> The resulting clusters that fell on the white matter were considered, and their volume was calculated. All results were manually verified to ensure their accuracy.

Lacunae were defined as “round or ovoid, subcortical, fluid-filled (similar signal as CSF) cavity, between 3 mm and 15mm in diameter”, according to Standards for Reporting Vascular Changes on Neuroimaging criteria.<sup>9, 10</sup> Lacunae had to be hypointense in T1-weighted images.

FLAIR and T2-weighted images were reviewed to ensure that those lesions identified as

lacunes on T1 had CSF-like signal. SWI MRIs were also reviewed to exclude the possibility of CMBs at these locations. Based on the location, we classified supratentorial lacunes as lobar (when located in CSO, frontal, parietal, insular/subinsular, temporal, and occipital lobes) or deep (when located in thalamus, basal ganglia, caudate, internal and external capsule).<sup>10</sup> Presence of any lacunes and total lacunes counts refer to presence and number of lacunes in any of the above-mentioned locations.

Thirty scans were reviewed by 2 trained raters (M.P and H.H.T, trained by reviewing a range of test cases based on the definitions) to assess the interrater agreement for the evaluation of MRI markers. The interrater agreement for detecting the SVD markers was good (lobar lacunes:  $k=0.73$ , 95% confidence interval [CI] 0.49–0.97; deep lacunes:  $k=0.76$ , 95% CI 0.50–1; lobar CMB:  $k=0.75$ , 95% CI 0.49–1; deep CMB:  $k=0.73$ , 95% CI 0.45–1; EPVS-CSO:  $k=0.74$ , 95% CI 0.50–0.98; EPVS-BG:  $k=0.80$ , 95% CI 0.59–1).

**PET analyses.** <sup>11</sup>C-PiB was synthesized in NTUH, and PET images (Discovery ST, GE Healthcare, Milwaukee, WI, USA) were acquired for 30 minutes approximately 40 minutes after injection of 10 mCi <sup>11</sup>C-PiB. The interval between the acquisition of PET and MRI scans were within 90 days in all patients. PET data were reconstructed with ordered set expectation maximization and corrected for attenuation. The PET data were semi-quantitatively analyzed and expressed as standardized uptake value ratios (SUVRs) of regions of interest using cerebellar cortex as the reference region as our group previously described.<sup>1</sup> The regions of interest included the frontal, temporal, parietal, and occipital lobes.

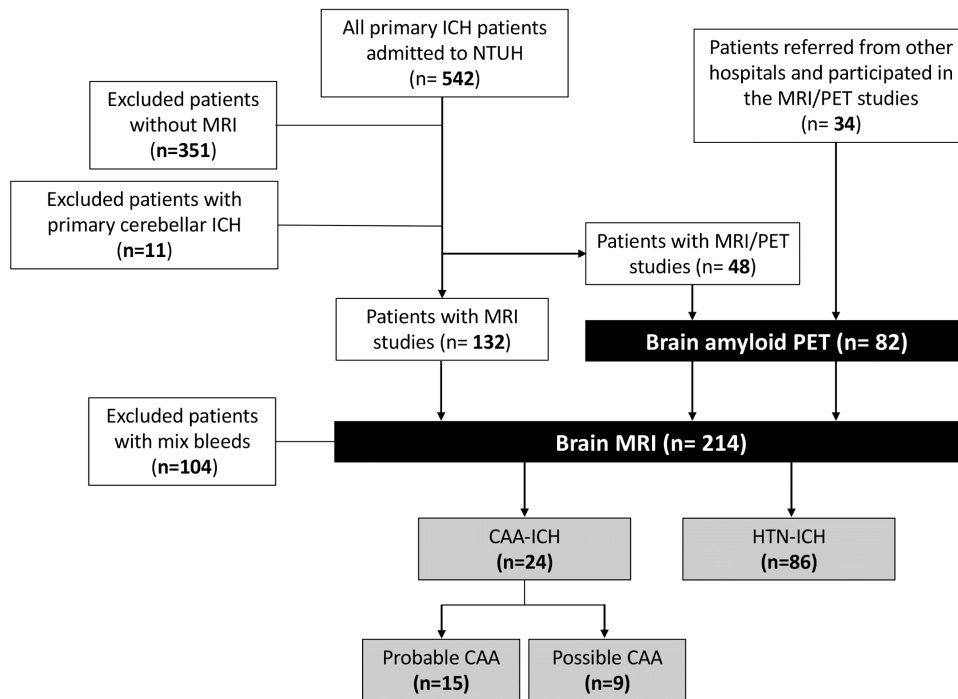
**Statistical analysis.** Categorical variables are presented as percentages, and the continuous variables are presented as mean  $\pm$  SD or median (interquartile range). In univariable analysis, we compared baseline demographics, clinical, and neuroimaging variables between the CAA-ICH and HTN-ICH groups as well as the lobar lacunes(+) and lobar lacunes(-) groups. Using a dichotomous dependent variable (presence or absence of lobar lacunes), multivariable logistic

regression models were built to look for independent associations between lobar lacunes and relevant neuroimaging markers of SVD including the following covariates: demographic and vascular risk factors (age, sex, hypertension), lobar CMB and WMH volume. The association between lobar lacunes count and cerebral PiB retention was performed using spearman's correlation analyses and partial correlation analyses adjusted for age. All statistical analyses were performed using SPSS version 22 (SPSS Inc., Chicago, IL). All tests of significance were 2-tailed with a threshold for significance of  $p < 0.05$ .

## Supplemental Reference:

1. Tsai HH, Tsai LK, Chen YF, Tang SC, Lee BC, Yen RF, et al. Correlation of cerebral microbleed distribution to amyloid burden in patients with primary intracerebral hemorrhage. *Sci Rep*. 2017;7:44715
2. Linn J, Halpin A, Demaerel P, Ruhland J, Giese AD, Dichgans M, et al. Prevalence of superficial siderosis in patients with cerebral amyloid angiopathy. *Neurology*. 2010;74:1346-1350
3. Yeh SJ, Tang SC, Tsai LK, Jeng JS. Pathogenetical subtypes of recurrent intracerebral hemorrhage: Designations by smash-u classification system. *Stroke*. 2014;45:2636-2642
4. Greenberg SM, Vernooij MW, Cordonnier C, Viswanathan A, Al-Shahi Salman R, Warach S, et al. Cerebral microbleeds: A guide to detection and interpretation. *Lancet Neurol*. 2009;8:165-174
5. Charidimou A, Boulouis G, Roongpiboonsopit D, Auriel E, Pasi M, Haley K, et al. Cortical superficial siderosis multifocality in cerebral amyloid angiopathy: A prospective study. *Neurology*. 2017
6. Charidimou A, Boulouis G, Pasi M, Auriel E, van Etten ES, Haley K, et al. Mri-visible perivascular spaces in cerebral amyloid angiopathy and hypertensive arteriopathy. *Neurology*. 2017;88:1157-1164
7. Iorio M, Spalletta G, Chiapponi C, Luccichenti G, Cacciari C, Orfei MD, et al. White matter hyperintensities segmentation: A new semi-automated method. *Front Aging Neurosci*. 2013;5:76
8. Fotiadis P, van Rooden S, van der Grond J, Schultz A, Martinez-Ramirez S, Auriel E, et al. Cortical atrophy in patients with cerebral amyloid angiopathy: A case-control study. *Lancet Neurol*. 2016;15:811-819
9. Wardlaw JM, Smith EE, Biessels GJ, Cordonnier C, Fazekas F, Frayne R, et al. Neuroimaging standards for research into small vessel disease and its contribution to ageing and neurodegeneration. *Lancet Neurol*. 2013;12:822-838
10. Pasi M, Boulouis G, Fotiadis P, Auriel E, Charidimou A, Haley K, et al. Distribution of lacunes in cerebral amyloid angiopathy and hypertensive small vessel disease. *Neurology*. 2017;88:2162-2168

**Supplementary figure I: Flowchart of patient enrollment and final study sample.**



**Supplementary Table I: Comparison of patients with and without lacunes.**

	<b>Lobar lacune (+)</b> (n=17)	<b>Lobar lacune (-)</b> (n=93)
Female, n (%)	7 (41.2%)	35 (37.8%)
<b>Age, mean (SD), y</b>	67.9 ± 15.9	60.7 ± 13.5*
Hypertension, n (%)	14 (82.4%)	88 (88.2%)
<b>CAA diagnosis, n (%)</b>	7 (41.2%)	17 (18.3%)*
Cerebral microbleed		
<b>Presence of lobar CMB, n (%)</b>	7 (41.2%)	8 (8.6%) <sup>§</sup>
Presence of deep CMB, n (%)	6 (35.3%)	39 (41.9%)
<b>White matter hyperintensity</b>		
<b>Fazekas scale ≥ 2, n (%)</b>	17 (100%)	55 (59.1%)*
<b>Volume, median (IQR), mL</b>	19.7 (8.6-37.3)	5.7 (1.6-19.1)*
Enlarged perivascular space		
CSO > 20, n (%)	8 (47.1%)	24 (25.8%)
BG > 20, n (%)	4 (23.5%)	18 (19.4%)
Cortical superficial siderosis, n (%)	1 (5.9%)	4 (4.3%)
	<b>Deep lacune (+)</b> (n=21)	<b>Deep lacune (-)</b> (n=89)
Female, n (%)	5 (22.7%)	37 (42.0%)
Age, mean (SD), y	66.4 ± 16.1	60.7 ± 13.4
Hypertension, n (%)	20 (90.9%)	76 (86.4%)
CAA diagnosis, n (%)	4 (19.0%)	17 (19.1%)
Cerebral microbleed		
Presence of lobar CMB, n (%)	3 (14.2%)	12 (13.4%)
<b>Presence of deep CMB, n (%)</b>	13 (61.9%)	32 (35.9%)*
<b>White matter hyperintensity</b>		
<b>Fazekas scale ≥ 2, n (%)</b>	18 (85.7%)	54 (60.7%)*
<b>Volume, median (IQR), mL</b>	19.3 (5.3-36.3)	7.9 (1.6-18.6)*
Enlarged perivascular space		
CSO > 20, n (%)	8 (38.1%)	24 (30.0%)
BG > 20, n (%)	7 (33.3%)	15 (16.9%)
Cortical superficial siderosis, n (%)	0 (0%)	5 (5.9%)

\*P-value < 0.05, §P-value < 0.001, all other comparisons not significant.

BG: Basal ganglia; CAA: Cerebral amyloid angiopathy; CMB: Cerebral microbleed; CSO: Centrum semiovale

**Supplementary Table II: Demographics and image characteristics in patients who had PiB scan.**

	CAA-ICH (n=15)	HTN-ICH (n=21)
Female, n (%)	8 (53.3%)	8 (38.1%)
<b>Age, mean (SD), y</b>	71.7 ± 12.8	60.1 ± 14.5*
<b>Hypertension, n (%)</b>	9 (60.0%)	19 (90.5%)*
Diabetes	2 (13.3%)	4 (19.0%)
Dyslipidemia, n (%)	1 (6.7%)	6 (28.6%)
LVH, n (%)	0 (0%)	1 (4.8%)
eGFR, mean (SD), mL/min/1.73m <sup>2</sup>	83.6 ± 13.3	82.4 ± 19.0
Previous ischemic stroke, n (%)	0 (0%)	3 (14.3%)
<b>Previous ICH, n (%)</b>	4 (26.7%)	0 (0%)*
Cerebral microbleed		
<b>Presence of lobar CMB, n (%)</b>	10 (66.7%)	0 (0%) <sup>§</sup>
<b>Presence of deep CMB, n (%)</b>	0 (0%)	9 (42.9%)*
White matter hyperintensity		
Fazekas scale ≥ 2, n(%)	12 (80.0%)	11 (52.4%)
Volume, median (IQR), mL	19.7 (7.9-27.9)	3.8 (2.6-19.3)
Cortical superficial siderosis, n (%)	2 (13.3%)	0 (0%)
Enlarged perivascular space (≥20)		
Centrum Semiovale, n (%)	6 (40%)	6 (28.6%)
Basal ganglia, n (%)	5 (33.3%)	6 (28.6%)
Presence of any lacune, n (%)	8 (53.3%)	7 (33.3%)
<b>Presence of lobar lacune, n (%)</b>	6 (40%)	2 (9.5%)*
Presence of deep lacune, n (%)	3 (20%)	6 (28.6%)
<b>PiB SUVR, median (IQR)</b>	1.26 (1.03-1.57)	1.09 (1.00-1.16)*

\*P-value <0.05, §P-value < 0.001, all others not significant.

CAA: Cerebral amyloid angiopathy; CMB: Cerebral microbleed; eGFR: Estimated glomerular filtration rate; HTN: Hypertension; ICH: Intracerebral hemorrhage; PiB: <sup>11</sup>C-Pittsburgh Compound B; SUVR: standardized uptake value ratio